View metadata, citation and similar papers at core.ac.uk
brought to you by CORE
provided by DSpace@MIT

Mechanics, Mechanisms and Modeling of the Chemical Mechanical Polishing Process

Kyungyoon Noh, Jiun-Yu Lai, Nannaji Saka, and Jung-Hoon Chun

Abstract— **The Chemical Mechanical Polishing (CMP) process is now widely employed in the Integrated Circuit Fabrication. However, due to the complexity of process parameters on the material removal rate (MRR), mechanism of material removal and pattern effect are not well understood. In this paper, three contact regimes between the wafer surface and the polishing pad were proposed: direct contact, mixed or partial contact, and hydroplaning. The interfacial friction force has been employed to characterize these contact conditions. Several polishing models are reviewed with emphasis on the mechanical aspects of CMP. Experiments have been conducted to verify the mechanical polishing models and to identify the dominant mechanism of material removal under typical CMP conditions.**

Keywords— **Chemical Mechanical Polishing, Process Control, Semiconductor Manufacturing, Integrated Circuits**

I. Introduction

THE ever-increasing demand for high-performance microelectronic devices has motivated the semiconductor industry to design and manufacture Ultra-Large-Scale Integrated (ULSI) circuits with smaller feature size, higher resolution, denser packing, and multi-layer interconnects. The ULSI technology places stringent demands on global planarity on the Interlevel Dielectric (ILD) layers and shallow trench isolation (STI). Compared with other planarization techniques, the Chemical Mechanical Polishing (CMP) process produces excellent local and global planarization at low cost, and is thus widely adopted in many back-end processes for planarizing multi-layer interconnects. The main objectives of CMP process are to smooth surface topography of dielectric deposits to enable multilevel metallization, and to remove excess coating material to produce inlaid metal damascene structures and shallow isolation trenches. However, due to the complexity of CMP by concurrent polishing of wide range of material and lumped parameter conditions, the process fundamentals for optimal process design and control and the basic material removal mechanisms in CMP are not yet well understood. The Preston equation is well known for its availability in CMP process and can be written as Eq. 1 [1].

$$\frac{dh}{dt} = k_p p v_R \tag{1}$$

where h is the thickness of the layer removed, t the polishing time, p the nominal pressure, v_R the relative velocity, and k_p a constant known as the Preston constant. In recent years, it has been demonstrated in many works that the above relation is also valid for metals and ceramics [2], [3].

Because of the material removal by mechanical, chemical, or chemomechanical interactions in the CMP process, an understanding of the contact condition at the wafer/pad interface is crucial to process characteriztion, modeling, and optimization. To date, however, there is no explicit methodology in the CMP literature to characterize wafer-scale interfacial conditions with process parameters. Some researchers have assumed that the wafer hydroplanes while being polished, and solved the Reynolds equation of lubrication layer [4], [5]. Another group has assumed the wafer is in contact, or partially in contact with the pad, and related the displacement of the wafer to the pad elastic modulus and solved the stress field by the classical contact mechanics model [6]. Due to the compliance of the pad material and that of the back film in the wafer carrier, direct measurement of the film thickness is unreliable. In this paper, accordingly, a systematic way of characterizing and monitoring the wafer/pad interfacial condition is proposed, and a theoretical framework for relating the process parameters to the different contact modes is established. Optimization scheme of the process for a stable interfacial condition and the design of a robust CMP process for reducing wafer-scale variation can be developed on the basis of this study.

Although the CMP applicability to achieve global planarity and to produce scratch-free surfaces have been proven during many years, the mechanisms of material removal are still not clearly understood. The various models including abrasion, melting, adhesion and chemical model developed so far, though significant, have only addressed partial aspects of the process [4]-[8]. In this paper, to understand the polishing mechanisms, several polishing models are developed and examined by experiment. Different

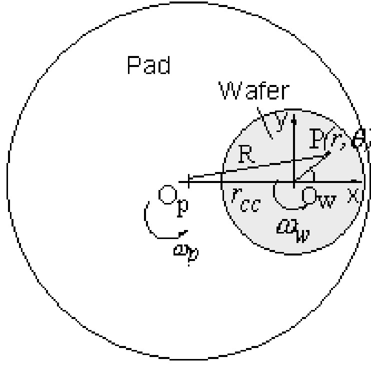

Fig. 1. Schematics of the coordinate systems for rotary polishers.

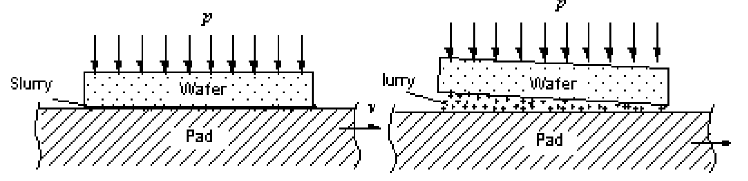

Fig. 2. Schematics of the wafer/pad interface at (a) contact and (b) hydroplaning mode.

aspects of the process, such as the material hardness, abrasive size, pad stiffness and its porous structure, are addressed and correlated with friction coefficient, material removal rate, Preston constant, and the wear coefficient. Finally, a process optimization scheme based on the models and experimental results is proposed.

II. MATERIAL REMOVAL CHARACTERIZATION

A. Kinematics

According to the rotary CMP machine type, the coordinate system for rotary polishers is shown in Fig 1. For the rotary polisher shown in Fig 1, the rotational centers of the wafer and the platen are O_w and O_p, and the angular velocities are ω_w and ω_p, respectively. The two rotational axes are normal to the polishing surface with an offset, r_{cc}.

The components of relative velocity of the wafer to the pad, $v_{r,R}$ and $v_{\theta,R}$, can be written as Eq. 2.

$$\begin{aligned} v_{r,R} &= -\omega_p r_{cc} \sin\theta \\ v_{\theta,R} &= \omega_w r - \omega_p (r + r_{cc}\cos\theta) \end{aligned} \tag{2}$$

The magnitude of the relative velocity is given as Eq. 3.

$$\begin{aligned} v_R &= [(\omega_p r_{cc} \sin\theta)^2 + (\omega_w r - \omega_p r_{cc}\cos\theta - \omega_p r)^2]^{1/2} \\ &= \{[(\omega_w - \omega_p)y]^2 + [(\omega_w - \omega_p)x - \omega_p r_{cc}]^2\}^{1/2} \\ v_{x,R} &= -(\omega_w - \omega_p)y; \quad v_{y,R} = (\omega_w - \omega_p)x - \omega_p r_{cc} \end{aligned} \tag{3}$$

When the angular velocities of the wafer and the platen are equal, i.e., $\omega_w = \omega_p$, Eq. 3 can be simplified as Eq. 4.

$$v_x = 0; \quad v_y = \omega_p r_{cc} \tag{4}$$

Thus, according to Eq. 4, the velocity of the wafer relative to the pad is in the y-direction only and is identical at all points on the wafer. But since the wafer rotates uniformly at a frequency of $\omega_w/2\pi$, this results in isotropic polishing. This setting was used in the experiments, because a uniform velocity simplifies the analysis and reduces the variation in material removal across the wafer as indicated by the Preston equation.

B. Characterization of Contact Mode

When the wafer is pressed against the polishing pad and sliding with an intervening fluid layer, the polishing slurry at the wafer/pad interface, the interfacial conditions can be characterized as: contact, hydroplaning and mixed mode.

B.1 Contact mode

In the contact mode, the asperities of opposing surfaces, wafer/pad or wafer/particle, mechanically interact. Usually, the real contact area is much smaller than the nominal surface area. Plastic deformation occurs on both surfaces at the contact spots. In the contact mode, the intervening fluid film is discontinuous and no significant pressure gradient will be formed in the fluid film across the diameter of the wafer to support the normal load. This type of contact mode occurs in the CMP practice when the relative velocity is low or the applied pressure is high. Since a tangential force is required to shear the surface asperities, the friction coefficient is relatively higher than that of the other two modes, usually on the order of 0.1. By assuming Coulomb friction in the contact mode at the scheme in Fig. 1, we can get a torque equation in Eq. 5.

$$Q_p = \iint \frac{\mu p r[-\omega_p r_{cc}^2 + (\omega_w - 2\omega_p) r_{cc} r\cos\theta + (\omega_w - \omega_p) r^2]}{[(\omega_w - \omega_p)^2 r^2 - 2\omega_p(\omega_w - \omega_p) r_{cc} r \cos\theta + \omega_p^2 r_{cc}^2]^{1/2}} d\theta dr \tag{5}$$

When $\omega_w = \omega_p$, the friction coefficient μ in the contact mode can be expressed as Eq. 6.

$$\mu = \frac{Q_p}{p\pi r_w^2 r_{cc}} \tag{6}$$

The friction coefficient in Eq. 6 may be affected by the materials of the wafer and the pad, their surface topographies, the presence of abrasive particles, the chemical composition, and so on. But, to a first approximation, the Coulomb friction coefficient is independent of the applied normal load, the relative velocity, the slight bowing or warping of the wafer, and the viscosity of the slurry fluid.

B.2 Hydroplaning mode

When the velocity is sufficiently high or the applied pressure is relatively low, the wafer will slide on a fluid film without directly touching the pad as shown in Fig 2. Because there is no contact between surfaces, the frictional force is due to the shear of the viscous fluid film, and the friction coefficient is expected to be much small, in the range 0.001 to 0.01, for typical hydroplaning conditions. Pressure builds up in the viscous fluid film to support the normal load on the wafer. In this mode, the normal load is no more supported by the pad asperities or the abrasive particles, but by the pressure in the slurry fluid film. The differential equation governing the pressure distribution in the fluid film is known as Reynolds equation. With the assumption that the "side-leakage" flow in the x-direction in Fig 1 can be neglected, a simplified one-dimensional Reynolds Equation can be obtained as Eq. 7

$$\frac{d}{dy}(h^3\frac{dp}{dy}) = 6\eta v_R \frac{dh}{dy} \tag{7}$$

where h is the slurry film thickness, p the pressure, and η the slurry viscosity. The normal load per unit width of the wafer in the x-direction, f_n, that the slurry film can support can be obtained by integrating the pressure function from inlet to outlet. Thus the frictional force per unit width due to fluid shear and the friction coefficient in the hydroplaning mode can be obtained as Eq. 8.

$$\begin{aligned} f_n &= \frac{6\eta v_R D^2}{(h_1-h_2)^2}[\ln(\frac{h_1}{h_2}) - \frac{2(h_1-h_2)}{(h_1+h_2)}] \\ f_t &= \frac{\eta v_R D}{(h_1-h_2)}[4\ln(\frac{h_1}{h_2}) - \frac{6(h_1-h_2)}{(h_1+h_2)}] \\ \mu &= \frac{f_t}{f_n} = \frac{\eta v_R}{p_{ave}(h_1-h_2)}[4\ln(\frac{h_1}{h_2}) - \frac{6(h_1-h_2)}{(h_1+h_2)}] \end{aligned} \tag{8}$$

Where h_1 and h_2 are the film thicknesses at the inlet and outlet, and D is the diameter of the wafer. The friction coefficient in Eq. 8 increases with slurry viscosity η and velocity v_R, and decreases with applied pressure. In the above analysis, the surfaces of the wafer and the pad are assumed to be smooth. In reality, this will only be true when the film thickness is much larger than the roughness of the pad so that the local topography of the pad surface will not affect the slurry flow. Moreover, a flat wafer surface is also assumed throughout the analysis although the wafer may be slightly curved. However, if the curvature is very small, similar results in terms of frictional force and friction coefficient will be obtained as those of a planar wafer surface. The friction coefficient for a typical CMP process can be estimated based on the above analysis and the value is about 0.004. Since this result is from the process parameters which most CMP processes operate, a low friction coefficient on the order of 0.001 is expected if the wafer is in the hydroplaning mode.

B.3 Mixed mode

As a transition from the contact mode to the hydroplaning mode, the mixed mode will occur when the velocity is increased or the pressure reduced. In this regime, the velocity is neither high enough nor the pressure low enough to build up a thick fluid layer to support the normal load. This will result in some contact between the pad asperities and the wafer surface. The friction force and the friction coefficient, therefore, are the weighted sum of the contact mode and hydroplaning mode and can be obtained as Eq. 9.

$$\mu = \alpha\mu_a + \beta\mu_p + [1-(\alpha+\beta)]\mu_l \tag{9}$$

where μ_a is the friction coefficient due to wafer/particle contact, μ_p that due to the wafer/pad contact, and μ_l that due to shear in slurry film and the constants α and β represent the fractional area in contact with the abrasive particles and the pad asperities.

C. Mechanisms of Material Removal

Over the decades, several models of polishing have been proposed. They include: surface melting, brittle fracture, microcutting, and burnishing. Each model emphasizes some fundamental mechanism of polishing and attempts to explain the phenomenon of material removal. Clearly, since a great number of variables are involved in polishing (e.g., materials, pressure and velocity on the specimen, polishing pads,

abrasive, and so on), a single mechanism is not expected to explain all aspects of polishing. Nevertheless, in what follows several analytical models are reviewed to elucidate the effects of certain process parameters on friction, material removal, and topography of polished surfaces. The present experimental results on wafer polishing are examined in the light of these models.

C.1 Surface Melting

When two surfaces slide relatively, most of the work done is converted into heat. In polishing, the heat is generated at the particle/surface contact area, which is a small fraction of the nominal area, and mostly diffuses through those contacts. A much higher temperature rise, or flash temperature, is expected at those contacts than in the bulk and may be sufficient to soften or even melt the surface. Wear occurs when the softened or melted material is smeared over the surface and eventually comes off the interface. The flash temperature T_f depends on the geometry of particle/wafer contacting area and the thermal conductivities of the sliding surfaces. In the steady state, T_f can be expressed as Eq. 10 [9].

$$T_f = T_0 + \frac{\mu f_n v_R}{2w} \frac{1}{k_1 + k_2} \tag{10}$$

where T_0 is the bulk temperature far away from the contact, μ the friction coefficient, f_n the normal load on the abrasive, v_R the relative sliding velocity, w radius of the circular contact region of a spherical abrasive particle, and k_1 and k_2 are the thermal conductivities of the coating material and the particle, respectively. The removal of material from the coating surface in the melting mode requires both that the flash temperature reaches the melting temperature and the melt form hot wear particles or a molten stream which will be consequently ejected form the interface. Although bulk temperature may rise with continued polishing, the circulation of slurry at the contact interface will remove larger part of the heat generated and keep the bulk temperature far below the melting point. Therefore, even the flash temperature reaches melting point, the melt will flow to the surrounding cool surface, and re-solidify without generating hot wear particles or squirting out as a molten stream. It may be concluded therefore that under typical CMP conditions, material removal by melting is not a viable mechanism.

C.2 Microcutting

In this polishing mode, abrasive particles act as single-point cutting tools and produce shallower and narrower grooves under the smaller load than those in grinding or other abrasion processes. Hardness determines the depth of particle penetration and, therefore, the material removal rate and surface finish. The abrasive is normally harder than the surface being polished to maintain a high rate of material removal. The frictional force is mostly due to the resistance of the soft surface being polished to plastic flow. Upper bound estimates for the friction coefficient and for material removal rate in the microcutting mode have been made in the past by idealizing the shape of the abrasive tip as a cone or a sphere. For a spherical tip, which is close to the shape of the abrasive particles, the friction coefficient, wear coefficient and surface roughness can be expressed as Eq. 11 [10].

$$\begin{aligned}
\mu &= \frac{2}{\pi}(\frac{2r}{w})^2\{\arcsin\frac{w}{2r} - \frac{w}{2r}[1-\frac{w}{2r}^2]^{1/2}\} \\
&+ 2\frac{s}{H}\{1-[1-(\frac{w}{2r})^2]^{1/2}\} \\
k_w &= \frac{2}{\pi}(\frac{2r}{w})^2\{\arcsin\frac{w}{2r} - (\frac{w}{2r}) + \frac{1}{2}(\frac{w}{2r})^3\} \\
R_a &\approx \frac{d}{2} = \frac{f_n}{2\pi r H}
\end{aligned} \tag{11}$$

Substituting the measured values of w and r in Eq. 11, μ and k_w are estimated to be 0.12 and 0.11, respectively. The friction coefficients, predicted by the microcutting model, for either cone or spherical abrasive, is close to the experimental values, about 0.15 - 0.22 for Cu. This suggests that the microcutting model explain, in part at least, the transmission of normal and shear stresses due to the action of the abrasive particle on the coating on a local scale. On the other hand, the estimated wear coefficient by the microcutting model, which ranges between 10^{-2} and 10^{-1}, is about two to three orders of magnitude higher than the experimental results 10^{-4}. The much smaller material removal implies that the material was not cleanly sheared off by a single pass of the abrasive particle. This point is also supported by the observation that no chip-like wear particles were found on the worn wafer or post-CMP pad surfaces. Instead, ridges were formed along with some deeper and wider grooves, which suggests particle plowing. Since the penetration depth in the CMP condition is usually very shallow, the attack angle for any shape of particles will be very small. Therefore, it is more likely that plowing will prevail rather than cutting. The smaller k_w also suggests that much of the work done by abrasive particles on the coating is to plastically deform the subsurface. The wear coefficient can be rewritten as Eq. 12 [11].

$$k_w = \frac{VH}{LS} = \mu\frac{VH}{\mu LS} = \frac{Vu}{FS} \tag{12}$$

where F is the tangential force on the wafer and u the specific energy, the work done to remove a unit volume of material. If cutting without plastic deformation is presumed, i.e. the plastic zone is limited to the grooved region, the specific energy is approximately equal to the hardness of the material being polished. Thus, based on Eq. 12, the wear coefficient might be interpreted as the ratio of work done by creating chips by cutting ($= Vu$) to the total external work done ($= FS$). When cutting is the dominant mechanism, most of energy is consumed to create chips and k_w should be close to unity. Since k_w is much less than unity in polishing, most of the external work is dissipated into the sub-surface region below the contact to create a large plastic deformation zone, deeper than the dimension of the grooves. Thus the microcutting model grossly overestimates the material removal rate. Nevertheless, for delineating the effects of important process parameters on the friction coefficient, wear coefficient, and surface roughness, the previous analyses is adequate to provide a qualitative picture of the polishing process.

C.3 Brittle Fracture

Fracture by plastic indentation occurs in brittle materials, such as glass, when the tip radius of the abrasive particle is below a critical value. In this small-scale contact, cracks are not induced in the elastic loading regime, but are observed with elastic/plastic penetration of particles. Lateral cracks initiate while the medium is unloaded and propagate parallel to the surface with repeat loading/unloading, and finally reach the surface and form wear particles. Cracks initiate when the load on the particle exceeds a transition threshold, f_n^* expressed as Eq. 13 [12].

$$f_n^* = \kappa(\frac{K_c^4}{H^3})f(E/H) \qquad (13)$$

where κ is a dimensionless constant, K_c the fracture toughness, H the hardness, and E the Young's modulus of the material being polished. For lateral cracks, $f(E/H)$ in Eq. 13 varies slowly with E/H and $\kappa f(E/H)$ is approximately 2×10^5. It is apparent that the critical load for both metal and ceramic coatings is many orders of magnitude greater than the load estimated earlier by particle penetration measurement, about $10^{-6}N$ for a typical CMP with 300 nm abrasive particles. Therefore, small particles employed in CMP generally prevent the initiation of cracks and the subsequent fracture. This again suggests that the prevailing mechanism of material removal is due to excessive plastic deformation.

TABLE I
Experimental conditions.

Experimental parameter	Value
Diameter of Wafer (mm)	100
Normal Load (N)	391
Normal Pressure (kPa)	48
Rotational Speed (rpm)	75
Linear Velocity (m/s)	0.70
Duration (min)	1-6
Sliding Distance (m)	42-252
Slurry Flow Rate (ml/min)	150
Abrasive	$\alpha - Al_2O_3$
Abrasive Size (nm)	300

C.4 Burnishing

Burnish, in which material is removed on a molecular scale, represents the least possible amount of wear. The wear coefficient can be as small as 10^{-8}. The mechanisms of burnish are not yet clear, and there is no direct observation to verify the hypothesis. It is proposed that material is removed molecule by molecule from the high spots by adhesive forces between the abrasive and surface material when the load is below a critical value. Therefore, the surface topography due to burnishing will be as smooth as that produced by evaporation. The wear coefficient reported for burnishing is about 10^{-8}, which is far below k_w, about 10^{-4}, in the polishing experiments. It suggests that burnishing, even if it occurs, is not the dominant material removal mechanism under CMP conditions.

III. EXPERIMENTAL

A. General

A rotary-type polisher was employed in the polishing experiments. The stainless steel wafer carrier was connected to a head motor by a gimbaling mechanism to align the wafer parallel to the platen surface. Two load sensors and a torque sensor were installed to measure the frictional forces in two orthogonal directions and the torque of the head motor. The capacities of the load and the torque sensors are 222 N and 5.65 Nm, and the resolutions are 0.067 N and 0.001 Nm, respectively. The head unit was driven by pneumatic pistons for vertical motion and for applying normal pressure. The platen unit is composed of a detachable 300 mm dia. aluminum platen and a platen motor. Surfaces of the aluminum platen and the base were ground to achieve a high degree of flatness and surface finish. Table 1 shows the general experimental parameters.

B. Contact mode characterization

Silicon wafer substrates, 100 mm in diameter, coated with 20 nm TiN as adhesion layer and 1 μm PVD Cu on the top were used as test wafers. A neutral slurry (pH = 7) with Al_2O_3 abrasive particles was used. The viscosity of the slurry was about . A commercial composite pad (Rodel IC1400) was employed in the polishing experiments. The pad comprised a microporous polyurethane top layer (Rodel IC1000) and a high-density urethane foam as underlayer. The room temperature elastic moduli of the top pad and the composite pad were about 500 MPa and 60 MPa, respectively.

C. Material removal mechanisms

All test specimens were in the form of 1 μm thick coatings on 100 mm dia. p-type (111) silicon wafers. The coatings include Al, Cu, SiO_2 (PECVD), SiO_2 (TEOS), and Si_3N_4. Two types of commercial polyurethane pads were used in present work. The Buehler CHEMOMET pad is a lighter, softer 1 mm thick pad composed of irregular, interconnected pores of an average diameter of 15 μm. The Rodel IC-1400 pad comprised two stacks. The top was a denser, stiff 1.3 mm thick stack with spherical, isolated pores of 40 μm in diameter. The average Material Removal Rate (MRR) of each coating was determined by weighing the wafer before and after polishing. For the SiO_2 coatings, the thickness was measured by ellipsometry at 49 fixed sites across the wafer to determine the local removal rate and the Within-Wafer Nonuniformity (WIWNU). The polished surfaces were examined in a Scanning Electron Microscope (SEM) and by an Atomic Force Microscope (AFM) to characterize surface roughness and surface scratches.

IV. RESULTS AND DISCUSSION

A. Contact mode characterization

A.1 Friction coefficient versus the parameter

Fig. 3 shows the effects of relative velocity and pressure on the friction coefficient. The relative velocities (0.05 to 3.91 m/s) and pressures (14 kPa and 48 kPa) employed in the experiments cover a wide range of practical CMP conditions. The friction coefficient is plotted in Fig. 3 against the parameter v_R/p. When v_R/p is small, i.e., at low velocity or high pressure, the friction coefficient is high and ranges between 0.40 and 0.49. As v_R/p increases, the friction coefficient falls from these values to 0.1 or lower. The transition points for the drop in friction for the two applied pressures are slightly off but are in a narrow range of v_R/p. After the transition, the friction coefficient seems to reach a minimum and then gradually

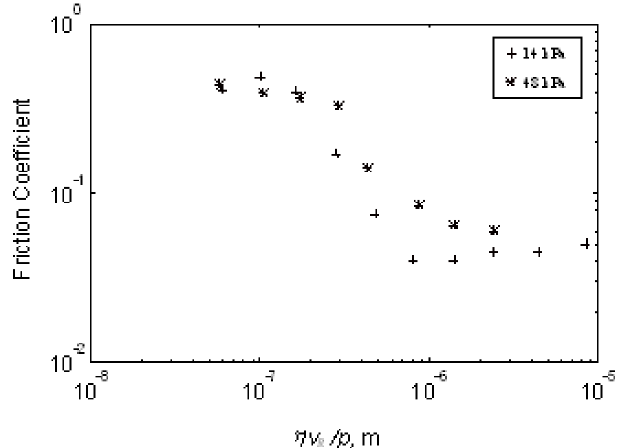

Fig. 3. The effect of the parameter on friction coefficient at the pressure of 14 kPa and of 48 kPa.

increase with v_R/p . The low friction coefficient values (especially at 14 kPa) are suspect since the friction force was too small to be measured by the load sensors on the experimental setup.

The experimental results show a consistent trend between the friction coefficient and the parameter v_R/p. For low v_R/p values, the friction coefficient is independent of both the applied pressure and the relative sliding velocity. Thus, the Coulomb friction law seems valid, and the high friction coefficients in the low v_R/p regime suggest that the wafer/pad interface is in the contact mode. After the transition point, the friction coefficient is no more independent of pressure or velocity. The friction coefficient decreases with the v_R/p, and the mixed mode regime sets in and lasts over an order of magnitude of the v_R/p value. However, the transition point from high to low friction is only slightly affected by the applied pressure. The full-fledged hydrodynamic mode, however, has not been realized for the experimental conditions chosen because the friction coefficients are far greater than 0.001.

A.2 Material removal rate and the Preston constant

As suggested by the Preston equation, Eq. 1, the material removal rate, MRR, can be plotted against the product pv_R but for better understanding of the effect of contact conditions, the normalized material removal rate, NMRR, and the Preston constant, k_p, are plotted in Fig. 4 against the dimensional parameter v_R/p, respectively. The Preston "constant" stays high at low v_R/p , i.e., in the contact mode, and drops down after the critical value, denoted as $(v_R/p)_c$. The experimental results show that the transition occurs around the same $(v_R/p)_c$ for both pressures.

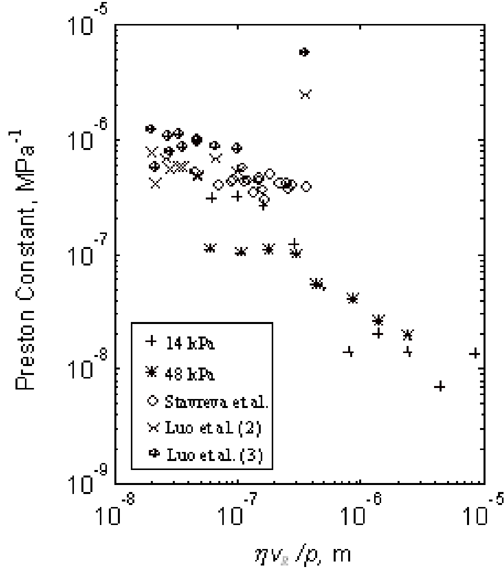

Fig. 4. The effect of the parameter on the Preston constant for Cu polishing.

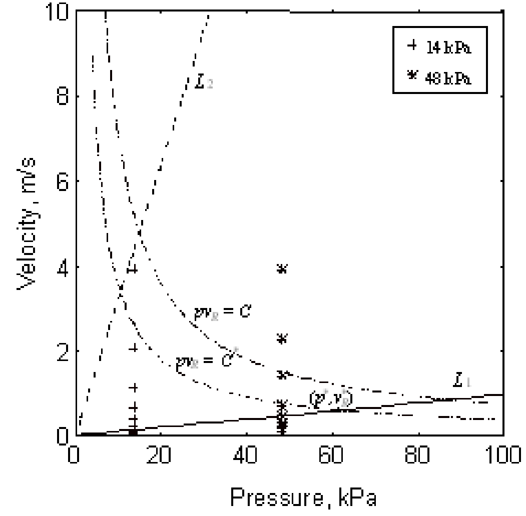

Fig. 5. Schematic of process optimization.

This implies that the Preston constant is independent of pressure and velocity when the wafer/pad interface is in the contact mode. After the transition point, the Preston constant decreases as v_R is increased or p decreased. It is also apparent that the Preston constant shows the same trend as that of friction coefficient. The variation of k_p can be explained in terms of the shifting interfacial conditions as follows. In the mixed mode, the friction coefficient decreases with v_R/p which implies that the wafer/pad contact area also decreases with v_R/p. The lack of contact further reduces the material removal rate since the fluid shear and the motion of the loose particles in the discontinuous fluid film cannot apply sufficient pressure on the wafer surface and remove material. With increasing v_R/p, particle rolling will increase and particle translation will decrease. In fact, some researchers tried to fit their data numerically to account for the variation of Preston "constant" at low pressure or high velocity conditions by a polynomial function of the pv_R product, or introduce extra pressure and/or velocity terms in Preston equation. They proposed that the interfacial shear stress and particle velocity will enhance the chemical reaction rate or mass transfer from the wafer surface. However, the variation in k_p might just be due to the varying interfacial contact modes as Fig. 4 shows and thus each contact mode is expected to have a different Preston constant.

A.3 Process optimization

The effects of the parameter v_R/p on the friction coefficient and the Preston constant provide an opportunity to optimize the CMP process. For a certain slurry viscosity, the different wafer/pad contact regimes can be delineated in the v_R-p space as shown in Fig. 5. Corresponding to the critical point $(v_R/p)_c$ for transition from contact mode to the mixed mode, a line L1 with the slope $(v_R/p)_c$ is drawn in Fig. 5 to represent the transition points for different pres1sures and velocities. The region bounded by L1 and the p-axis represents the contact mode. Similarly, another line, L2, with a greater slope to represent the transition from the mixed mode to the hydroplaning mode is drawn. The region bounded by L2 and the v_R-axis represents the hydroplaning mode. The region bounded by L1 and L2 represents the mixed mode. For CMP process optimization, two wafer-scale requirements, material removal rate (MRR) and within-wafer non-uniformity (WIWNU), should be simultaneously satisfied. Thus a high Preston constant regime should be chosen for high MRR. This corresponds to the contact regime below line L1 in Fig. 5, where the Preston constant is high and independent of both p and v_R. From the viewpoint of reducing WIWNU also, contact mode is preferable with since the wafer/pad contact interface is more stable than the hydroplaning mode or the mixed mode and the velocity is uniform over the entire surface of the wafer.

From Eq. 1, the pv_R product should be as high as possible to increase the MRR, i.e., the highest velocity available is preferable in the contact regime for

a given pressure and vice versa. This suggests that the optimal conditions are located on the line L1. However, a high pressure requires a sturdy machine structure, which generally sets an upper limit for the applicable pressure. Besides, at a high pressure even a small vibration of the machine might result in large fluctuations on the normal load and friction force at the wafer/pad contact interface, and thus increase the WIWNU. These considerations suggest that the pressure increase cannot be unlimited. Similarly, extremely high velocities are not desirable because it is difficult to retain the fluid slurry on the platen at high velocities.

B. Material removal mechanisms

Based on the optimization scheme in section A.3, the v_R/p ratio should be chosen such that the wafer/pad interfacial condition remains in the contact regime. And the optimal pv_R product is also constrained by the heat generation and the WIWNU specification. Thus the key to enhance MRR is to increase the k_p or k_w. The MRR, NMRR and Preston constant are inversely proportional to the hardness of the coatings as shown in Fig. 6. The wear coefficient is about 10^{-4}, for the materials polished.Comparing the theoretical estimates and experimental results, the two-orders-of-magnitude gap of k_w provides an opportunity for process improvement: it might be possible to increase the k_w without a significant increase of surface roughness by encouraging the mode of material removal from plowing toward microcutting. As discussed earlier, a larger size of particle can be employed to increase the k_w; however, the tradeoff of using larger abrasive is the increase surface roughness and the scratch size and density as shown in Fig. 7. The MRR, or k_w in this case due to the constant pv_R, increases about 2.6 times whereas the roughness remains at a low level when the particle size is increased from 50 nm to 1000 nm. Even larger particles might be employed in the future to find the optimal size. In addition, the pH value of the slurry can be adjusted to increase the MRR for specific material. It has been reported that MRR of SiO_2 increase dramatically at high pH values, higher than 11, and MRR of Cu can be enhanced at a moderate acidic slurry, around 4.2. It is believed that changing pH value will change the hardness of the coating so as to affect the MRR and k_w.

Another scheme to increase k_w might rely on preventing the particle rolling, in which the particle/pad interfacial friction coefficient and the contact area must increase. The frictional coefficient between the abrasive particle and the pad depends on the adhesion of those two materials, and the particle/pad contact area at a given load can be increased by choosing a soft pad material. However, according to the previous analyses, the decrease of pad hardness will increase the wafer/pad contact area and reduce the load distributed on the particle, and thus reduce k_w. An appropriate pad material with good adhesion to abrasive particles, or even like fixed abrasive lapping paper, with a sufficient hard surface layer might be used to increase the sliding and the load distributed on the particles to increase MRR and k_w.

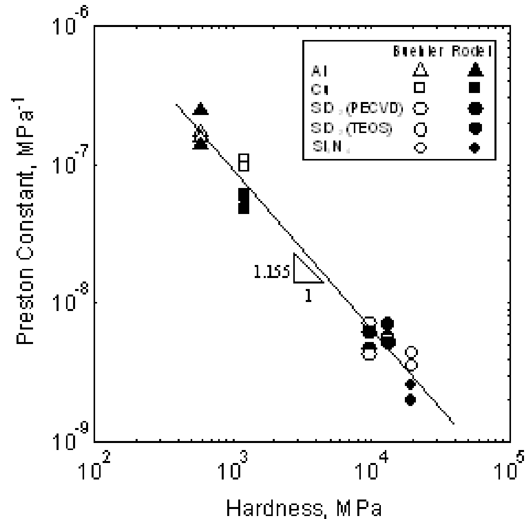

Fig. 6. Effect of coating hardness on Preston constant with 300 nm abrasive.

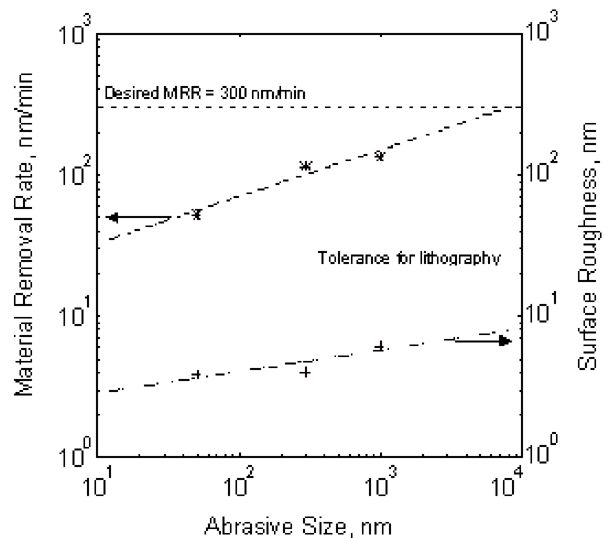

Fig. 7. Process optimization scheme by emploing the abrasive size effect (on Cu wafers).

V. CONCLUSIONS

• Three wafer/pad contact conditions - contact, hydroplaning, and mixed modes - may be proposed for the CMP process. Models for identifying each mode based on the friction coefficient have been formulated. The friction coefficient varies by one or two orders magnitudes among the different contact modes since the resistance to wafer motion could change by orders of magnitude in the presence of a thin slurry film. Typically, the friction coefficient for contact mode will be on the order of 0.1, for mixed mode on the order of 0.01 to 0.1, and for full-fledged hydrodynamic mode it will be 0.001. This wide range in friction suggests that friction coefficient can be used as an effective indicator to monitor the contact conditions in the CMP process. Experiments on Cu blanket wafers with neutral Al_2O_3 slurry have been conducted to verify the models for a wide range of pressure and velocity settings. The results suggest that the CMP process must be operated in the contact mode. Hydroplaning is not a stable process mode in terms of the gimbaling point location, wafer curvature, and fluctuations in slurry flow. Accordingly, the important issue in CMP process design is to select process parameters to maintain the process in the stable contact regime.

• The effects of process parameters on the material removal rate, and the relations between the friction coefficient and Preston constant are examined. The results show that Preston constant is independent of the pressure and velocity only in the contact regime. Moreover, the high correlation between the friction coefficient and Preston constant in the contact mode suggests the possibility of using friction coefficient to monitor the material removal rate in CMP. Further study on the polishing mechanisms and the role of chemistry in CMP is required to determine the correlation between the friction coefficient and the Preston constant, and the material removal rates.

• Theories of polishing processes - surface melting, plastic deformation, brittle fracture and burnishing - have been reviewed. Each theory was examined for friction coefficient, material removal rate, Preston constant, wear coefficient, and the topography of the worn surface. Based on the experimental results, the friction coefficient remains at a low and constant level, around 0.1 - 0.3. It is close to the value predicted by the plastic deformation model. Thus, the prevailing mechanism of material removal in fine abrasive polishing is plastic deformation. Surface melting does not occur because the temperature rise is marginal. Brittle fracture has not been observed because the normal load on the abrasive particle is below the critical value for fracture. Moreover, burnishing does not play a significant role in removing material since the work of adhesion is extremely low.

• The MRR, NMRR and Preston constant are inversely proportional to the hardness of the coatings. The wear coefficient is about 10^{-4}, for the materials polished. The microcutting model yields a higher value of MRR and wear coefficient (10^{-2}) than those of experiments. This discrepancy is explained on the basis of the small penetration depth of the particle, due to the small abrasive employed, the lighter load on the abrasive, due to the wafer/pad direct contact, and particle rolling. Stiffer pad results in a better wafer-scale uniformity, or a lower WIWNU and The size-effect of the abrasive is employed to increase the MRR and wear coefficient. The MRR increases about 2.6 times with the increase of particle size from 50 nm to 1000 nm. The surface roughness however increases at a slower rate, about 1.6 times, and remains below an acceptable level, about 20 nm.

Acknowledgments

The authors would like to acknowledge the support from the Singapore-MIT Alliance Program.

References

[1] Preston, F.W., *The Theory and Design of Plate Glass Polishing Machines,* J. Soc. Glass Technology , 11: 214-256l, 1927.

[2] Steigerwald, J.M., Zirpoli, R., Murarka, S.P., Price, D., Gutmann, R.J., *Pattern Geometry Effects in the Chemical-Mechanical Polishing of Inlaid Copper Structures,* J. Electrochem. Soc., 141: 2842-2848. 1994.

[3] Stavreva, Z, Zeidler, D., Plotner, M., Grasshoff, G., Drescher, K., *Chemical Mechanical Polishing of Copper for Interconnect Formation,* Microelectronic Engr., Vol. 33, pp. 249-257, 1997.

[4] Runnels, S.R., *Tribology Analysis of Chemical-Mechanical Polishing,* J. Electrochem. Soc., Vol. 141, pp. 1698-1701, 1994.

[5] Sundararajan, J.M., Thakurta, D.G., et al, *Two-Dimensional Wafer Scale Chemical Mechanical Planarization Models Based on Lubrication Theory and Mass Transport,* J. Electrochem. Soc., Vol. 146, pp. 761-766, 1999.

[6] Chekina, O.G., Keer, L.M., and Liang, H., *Wear-Contact Problems and Modeling of Chemical Mechanical Polishing,* J. Electrochem. Soc., 145: 2100-2106, 1998.

[7] Brown, N.J., Baker, P.C., and Maney, R.T, *Optical Polishing of Metals,* Proc. SPIE, Vol. 306, pp. 42-57, 1981.

[8] Cook, L.M., *Chemical Process in Glass Polishing,* J. Non-Crystalline Solids, Vol. 120, pp. 152-171, 1990.

[9] Jaeger, J.C., *Moving Sources of Heat and the Temperature at Sliding Contacts,* J. Proc. Royal Soc. N. South Wales, Vol. 76, pp. 203-224, 1942.

[10] Komvopoulos, K., Saka, N., Suh, N.P., *The Mechanism of Friction in Boundary Lubrication,* ASME J. Tribology, Vol. 107, pp. 452-461, 1985.

[11] Holm, R., *Electric Contacts,* Almqvist and Wiksells, Stockholm, 1946.

[12] Evans, A.G., Marshall, D.B., *Wear Mechanisms in Ceramics,* Fundamentals of Friction and Wear of Matreials,

ASM, pp. 439-452, 1980.

Kyungyoon Noh is a Ph.D student in Mechanical Engineering at MIT. His research interests include the characterization and process control of oxide and copper CMP process. He earned his bachelor's and master's degree in the Mechanical Design and Production Engineering from Seoul National Univeristy in 1995 and 1997.

Jiun-Yu Lai earned his doctoral degree in Mechancial Engineering at MIT in 2001 and is now working at Intel. His research focuses on the characterization and modeling of copper CMP process.

Nannaji Saka is Senior Research Scientist in Mechanical Engineering at MIT. He earned his doctoral degree in Materials Science and Engineering at MIT in 1974 and over the years, he has collaborated with Prof. Suh, Prof. Chun and other ME faculty on a variety of manufacturing processes, such as powder metallurgy, solidification processing, and Chemical Mechanical Polishing (CMP).

Jung-Hoon Chun is Professor of Mechanical Engineering and co-director of the Manufacturing Institute at MIT. He has been a member of the MIT Mechanical Engineering faculty since 1989, and is involved in several research area of innovative materials processing and manufacturing. As a part the International 70-nm Initiativem he is currently involved in the development of next-generation processes and equipment for the semiconductor industry including chemical-mechanical polihing (CMP) and photo-resist coating. His uniform droplet spray (UDS) apparatus, developed to study droplet-based manufacturing (DBM) processes, has been widely used in the electronics packaging industry.